Supplemental Material for

# Active motion of multiphase oil droplets: emergent dynamics of squirmers with evolving internal structure

Xin Wang,[1,‡] Rui Zhang,[2,4,‡] Ali Mozaffari,[2] Juan J. de Pablo,[2,3] Nicholas L. Abbott[1,*]

[1]Smith School of Chemical and Biomolecular Engineering, Cornell University, Ithaca, New York 14850, USA

[2]Pritzker School of Molecular Engineering, University of Chicago, Chicago, Illinois 60637, USA

[3]Center for Molecular Engineering, Argonne National Laboratory, Lemont, Illinois 60439, USA

[4]Current address: Department of Physics, The Hong Kong University of Science and Technology, Clear Water Bay, Kowloon, Hong Kong, China.

**Additional comments on past studies of nematic droplets.** We note that past studies have reported that high TTAB concentrations (*e.g.*, 250 mM) can lead to curly motions of single phase nematic droplets due to an interplay between convective flow and the elasticity of the internal nematic phase[1,2]. In our experiments, we used a low TTAB concentration (100 mM)[2] that, as discussed in the main text, does not generate viscous stresses sufficient to break the symmetry of single phase nematic droplets.

**Additional comments on negative autochemotaxis that lead to oscillation of droplet velocity.** Negative autochemotaxis is an effective repulsion acting between a droplet and it previous trajectory[3]. In our study, the autochemotactic effect reflects the presence of oil-swollen micelles along the droplet trajectory, thus causing deceleration of a droplet when it approaches its past trajectory and acceleration of the droplet when moving away from the previous trajectory. Inspection of Fig. 4d also reveals that the changes in velocity with time become less abrupt with each recrossing of the droplet trajectory, consistent with diffusive broadening of the concentration profile of oil-swollen micelles in the wake left behind the droplet.

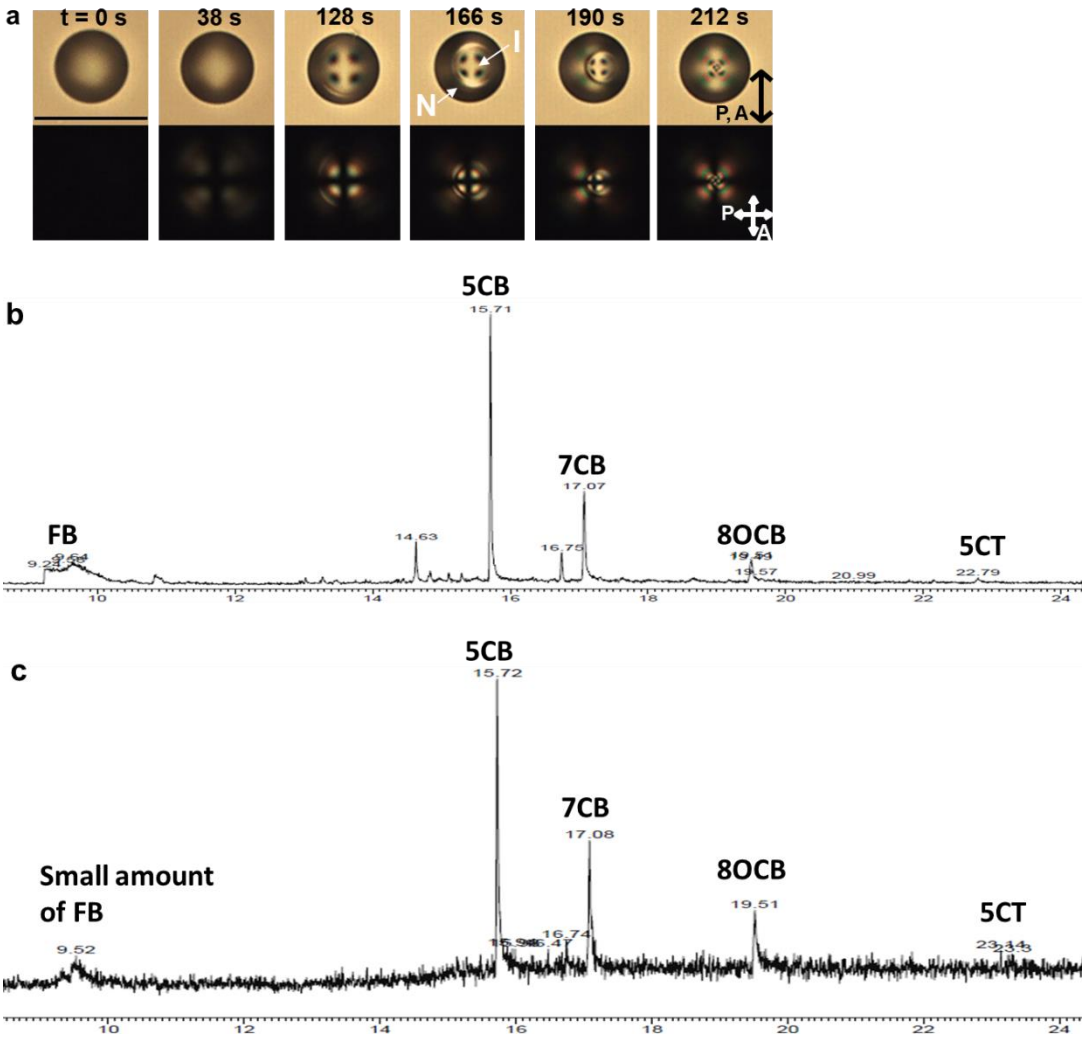


**Fig. S1. Preferential extraction of perfluorobenzene (FB) from emulsion droplets prepared from mixtures of FB and E7.** (a) Phase transition from isotropic to nematic phase during extraction of a droplet at 58 ºC in 100 mM TTAB micellar solution. Scale bar, 50 μm. Gas chromatogram showing the composition of droplets (b) before and (c) after the solubilization process in the TTAB solutions. 5CB, 7CB, 8OCB and 5CT are the four components of the E7 liquid crystalline mixture.

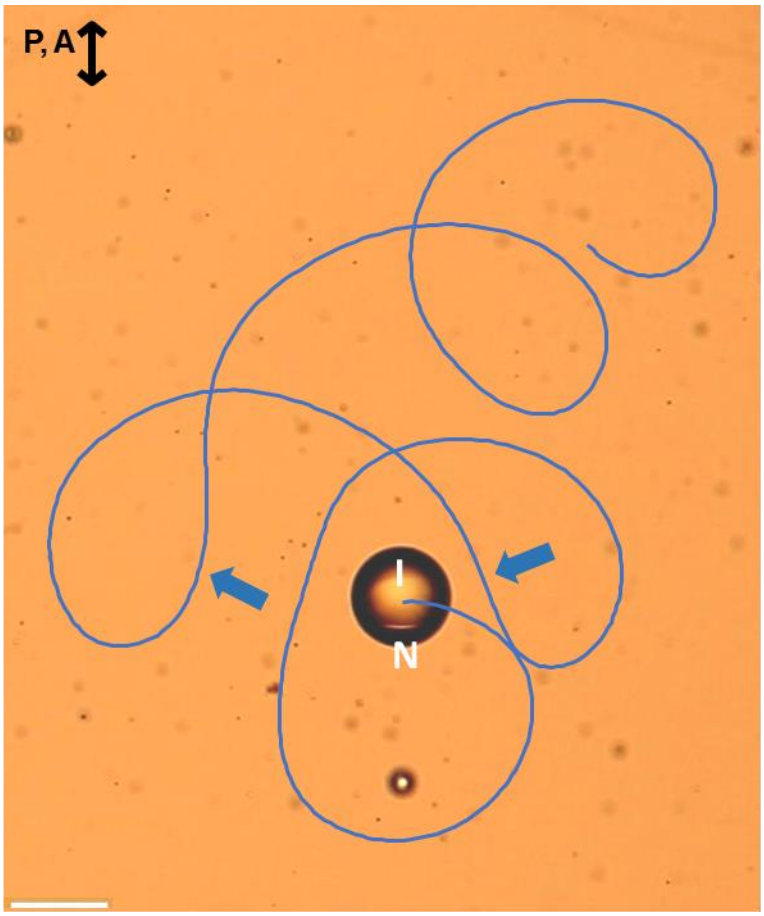


**Fig. S2. Trajectory during which the handedness of the spiralling motion switched sign (denoted by blue arrows).** Scale bar, 50 μm. This switch was observed more frequently with droplets with sizes (~30 - 40 μm) that were small compared to the aqueous film thickness (~100 μm, Z-axis), suggesting that hydrodynamic interactions with the confining surfaces suppress switching.

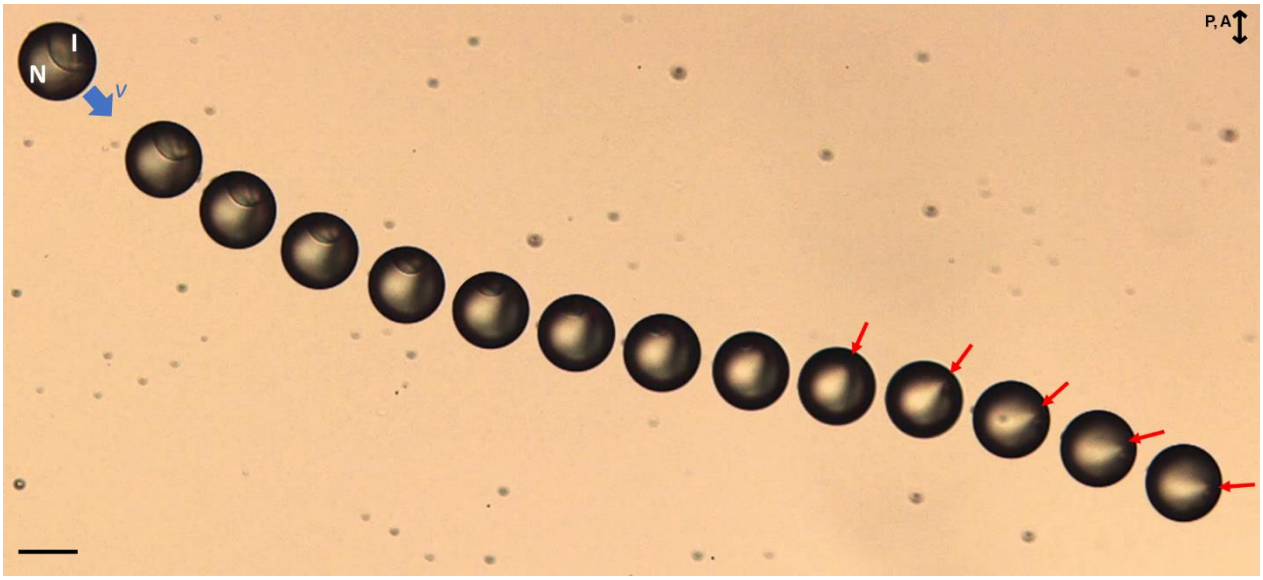


**Fig. S3. Reorganization of the internal morphology of droplet during the transition from State IV to V dynamical states.** Time-lapse micrographs show that the defect (denoted by red arrows) is convected to the leading edge during the transition from State IV to State V. Scale bar, 50 μm.

We have explored the phase behavior of perfluorobenzene (FB) and E7 in a prior publication (ref. 30). For the convenience of readers, we show a schematic illustration of the phase diagram (Fig. S4a, temperature vs. concentration of FB in LC). To observe the spiraling motion, the oil phase in the droplet must be in the N+I coexistence region. Oil compositions that exhibit N+I coexistence at low temperature, *e.g.*, mixture (i) in Fig. S4a, have an overall higher FB concentration compared to oil compositions that exhibit N+I coexistence at high temperature, *e.g.*, mixture (ii) in Fig. S4a. The low concentration of FB at high temperature will lead to a low rate of solubilization and thus low propulsive velocity and long rotational period. We note that we have measured the droplet velocity to depend on FB concentration (Fig. S4b, droplet velocity decreases as a function of time, *i.e.*, with decrease in FB concentration).

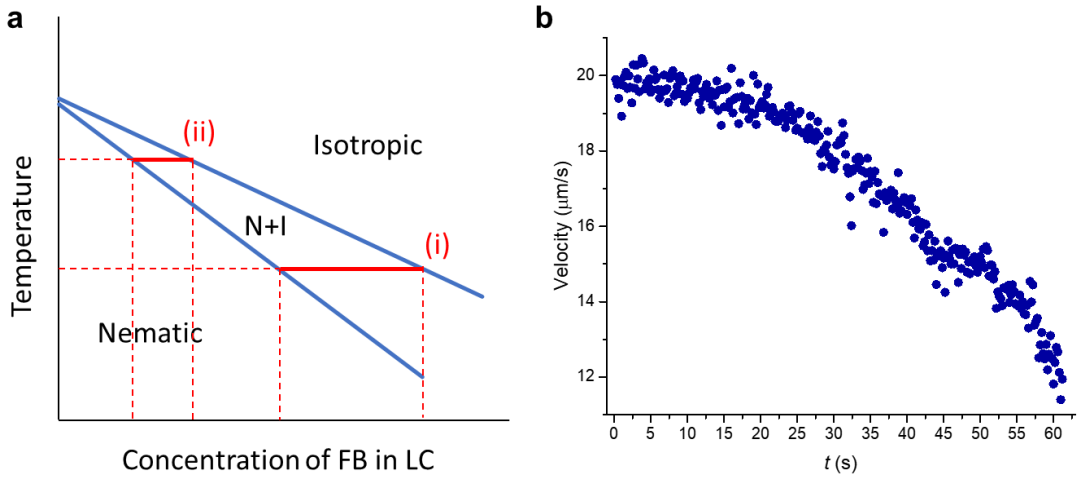


**Fig. S4.** (a) Schematic illustration of the phase diagram of the LC+FB oil phase. (b) Velocity of a nematic single phase droplet comprising a LC-FB mixture. The velocity deceases as a function of time (*i.e.*, with decrease in FB concentration).

The droplet behaviors described in Fig. 1 are driven by a phase transition (isotropic to nematic) that accompanies solubilization of select components of the oil mixture at constant temperature. This change in composition is depicted as process (1) in Fig. S5. As reported in the main text, after the isothermal solubilization process had resulted in formation of a nematic droplet (ending at point A in Fig. S5), we increased the temperature, causing the nematic oil mixture to transform back into an isotropic phase again (process (2) in Fig. S5). After the thermal phase transition, we allowed the solubilization experiment (process (3)) to again transform the isotropic droplet into a nematic droplet. This process was repeated up to 5 times in our system.

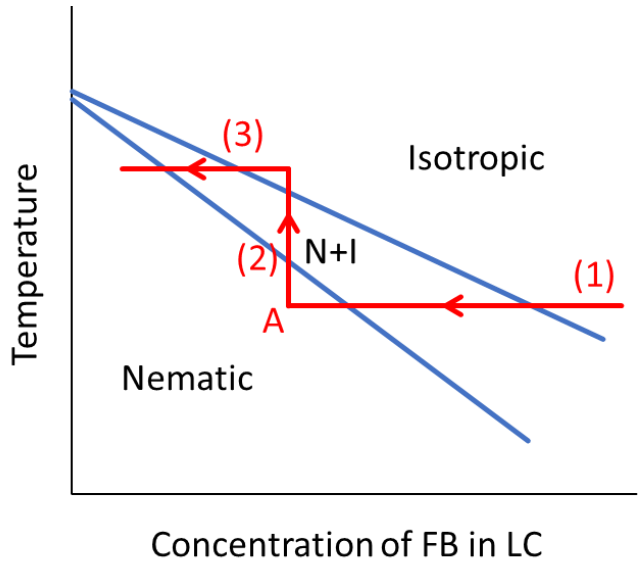


**Fig. S5**. Schematic illustration of the phase diagram of the LC+FB oil phase.

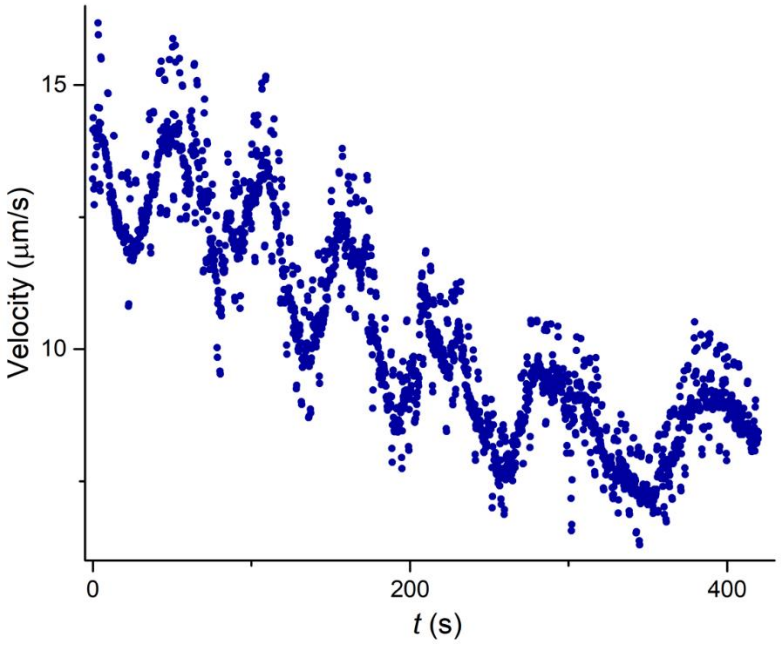


**Fig. S6. Velocity of droplet motion during State III** showing oscillations due to autochemotaxis while spiralling (re-crossing of trajectory).

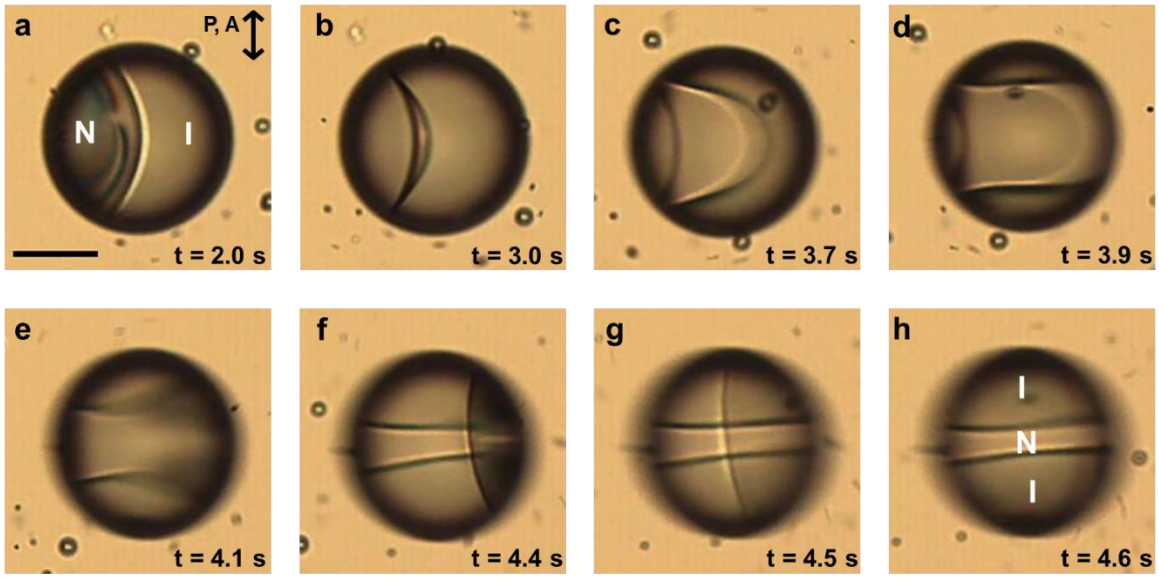


**Fig. S7. Reconfiguration of droplet morphology with external concentration gradient of TTAB.** Time-lapse micrographs showing the isotropic domain of a Janus droplet (isotropic and nematic domains) breaking up into two lobes when moving to the right following an external TTAB gradient. Scale bar, 50 μm. We used SDS in Fig. 5 of the main text for ease of visualization because SDS generates a slower surface flow enabling formation of a steady state before the droplet reached the edge of the glass optical cell.

**Supplementary Video 1:** Movie showing a Janus droplet transitioning from ballistic (State II, puller) to spiraling (State III, neutral squirmer) and back to ballistic (State IV, neutral squirmer) motion, with orientation of internal interfaced between compartments changing as indicated in Fig. 1 and Supplementary Video 2.

**Supplementary Video 2**: Movie showing the inner interface of a Janus droplet reorienting from perpendicular to parallel to the direction of motion during the transition from puller (State II) to neutral squirmer (State III).

**Supplementary Video 3**: Movie showing that spiraling motion (State III) of the droplet can be reversed back to ballistic motion (State II) by increasing temperature by 1 $^{o}$C.

**Supplementary Video 4**: Movie showing how tracer particles are used to quantify the flow field near the surface of the self-propelled droplets. The droplet shown is undergoing a spiraling motion (State III), with an isotropic domain on the left and a nematic domain on the right compartment of the droplet. The displacement of the tracer particles reveals a higher flow rate near the isotropic surface (40 μm) versus nematic surface (9 μm) of the droplet.

**Supplementary Video 5**: Movie showing the motion and morphological reconfiguration of droplets in an external surfactant gradient, as described in Fig. 5.

1. Krüger, C., Klös, G., Bahr, C. & Maass, C. C. Curling Liquid Crystal Microswimmers: A Cascade of Spontaneous Symmetry Breaking. *Phys. Rev. Lett.* **117,** 048003 (2016).
2. Suga, M., Suda, S., Ichikawa, M. & Kimura, Y. Self-propelled motion switching in nematic liquid crystal droplets in aqueous surfactant solutions. *Phys. Rev. E* **97,** 062703 (2018).
3. Jin, C., Krüger, C. & Maass, C. C. Chemotaxis and autochemotaxis of self-propelling droplet swimmers. *Proc. Natl. Acad. Sci. U. S. A.* **114,** 5089–5094 (2017).